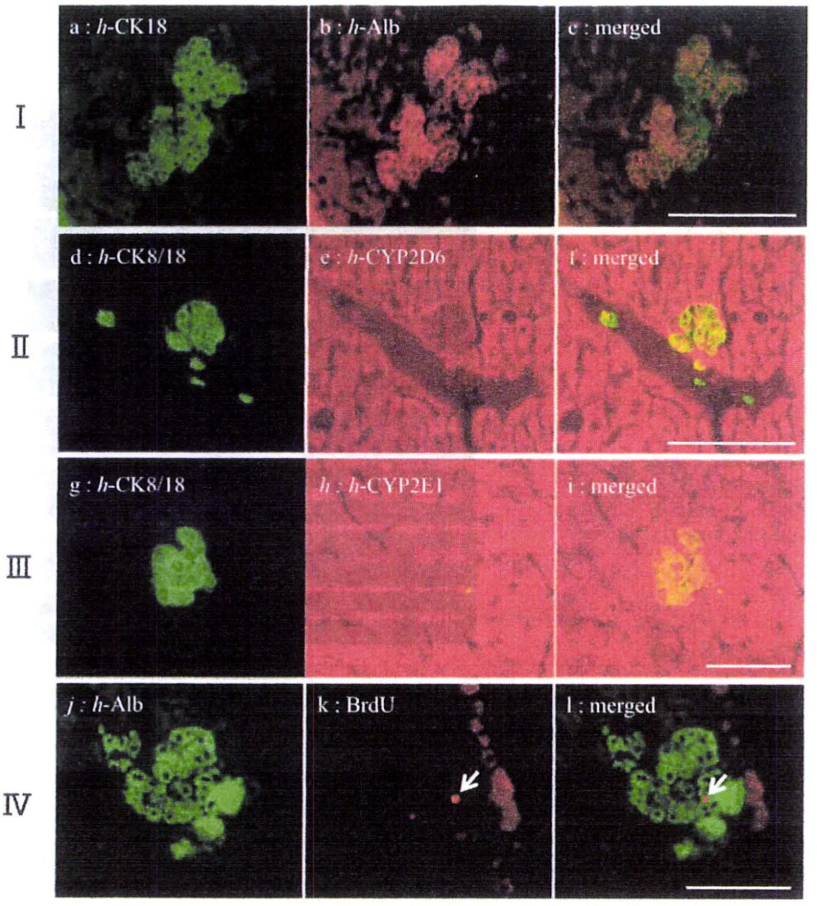

Fig. 4. Characterization of *h*-hepatocytes in the host liver. The rat liver was harvested at 4 weeks post-*h*-HPCT. Some animals were given BrdU 1 h before harvesting. These livers were processed to histological examinations. Four sections (sections I–IV) are presented here. The sections I and IV were formalin-fixed paraffin-processed for *h*-CK18, *h*-Alb, and BrdU staining. The sections II and III were cryo-processed for *h*-CK8/18, *h*-CYP 2D6, and *h*-CYP2E1. The section I was subjected to double immunostaining for *h*-CK18 (a) and *h*-Alb (b). Section II: double immunostaining for *h*-CK8/18 (d) and *h*-CYP 2D6 (e). Section III: double immunostaining for *h*-CK8/18 (g) and *h*-CYP2E1 (h). Section IV: double immunostaining for *h*-Alb (j) and BrdU (k). Images c, f, i, and l are merged photographs of a and b, d and e, g and h, and j and k, respectively. Scale bar = 20 μm.

consistently observed that immunosections of the group with *h*Alb > 15 ng/ml showed the distributions and the size of the *r*- and *m*-macrophages similar to those depicted in Fig. 5b as shown in Fig. 5c in which the liver of rat #5 is presented as a representative example. In contrast, $BM8^+$-*m*-macrophages became larger in size in the liver of the group with *h*Alb > 15 ng/ml as shown in Fig. 5d in which an immunosection from rat #6 is presented. We quantified the red colored areas (*m*-macrophage areas) in the photos shown in Fig. 5c,d as a measure of cell size using an image analyzer. The average red area per unit measured area of the rat with with *h*Alb > 15 ng/ml was ~3-fold larger than that with *h*Alb < 10 ng/ml. It is generally accepted that macrophages become enlarged when activated. Therefore, assuming that a *h*Alb concentration < 10 ng/ml predicts that the *h*-hepatocytes will not survive due to rejection by the host, we propose that macrophage activation limits the proliferation and survival of *h*-hepatocytes in SCID rats. The blood *h*-Alb concentration of rat #1 was relatively high (~95 ng/ml) at 3 weeks post-*h*-HPCT, but dropped to < 10 ng/ml at 4 weeks post-*h*-HPCT, most probably due to the rejection of *h*-hepatocytes.

Discussion

We are able to generate reproducibly, and in a stable form, SCID mice with livers that comprise mainly *h*-hepatocytes [3]. Several such immunodeficient and liver-injured mice have been used as hosts for the repopulation of *h*-hepatocytes, including uPA/SCID/beige mice [12], uPA/SCID mice [3,13], recombination activation gene 2 (*Rag-2*) knockout (KO) mice [14], and Fah KO/Rag2KO/IL2RγcKO mice [15].

In the present study, we explored the possibility of creating immunodeficient rats that are suitable for *h*-hepatocyte transplantation. Initially, we irradiated nude rats with X-rays, to eliminate their BMCs, and we then transplanted *m*-BMCs into the rats. Irradiation with the optimal regimen (10 + 10) allowed the m_{SCID}-BMCs to replace almost completely the *r*-PBMCs (the replacement rate of mouse MHC class I cells was 94%) at 5 weeks post-*m*-BMCT. The obtained SCID rats

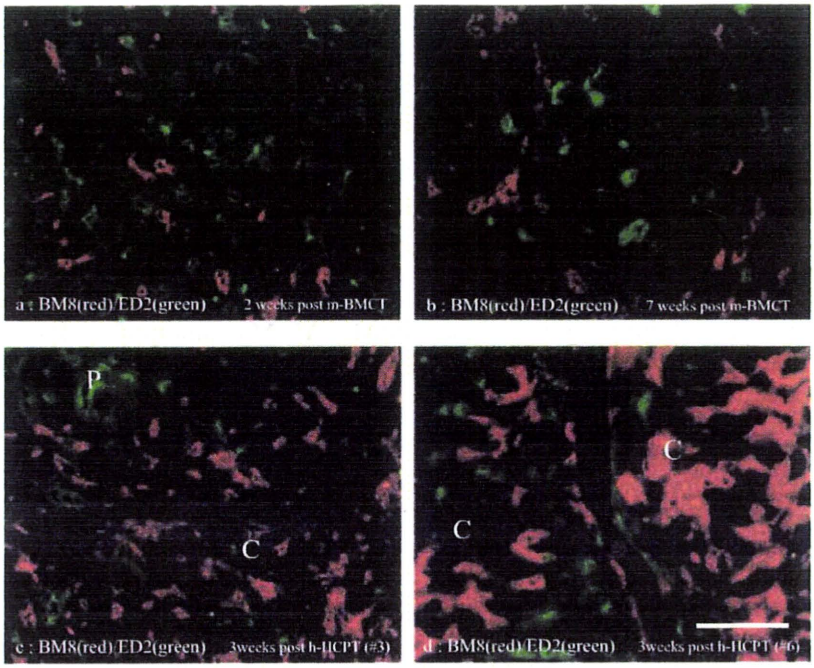

Fig. 5. Distributions of *r*- and *m*-Kupffer cells in the host livers. a and b. Six F344 nude rats were subjected to X-ray irradiation and transplanted with m_{SCID}-BMCs. Rat liver tissues were harvested at 2 weeks (a) and 7 weeks (b) post-*m*-BMCT from three animals each and double-immunostained for the detection of *m*- and *r*-macrophages using the BM8 (red) and ED2 (green) antibodies, respectively. The staining patterns for these antibodies are similar throughout the liver. Similar staining patterns were observed among the animals at each time point. c and d. Liver cryosections from 7 rats (#1–8 except #7) shown in Fig. 2 were prepared at 4 weeks post-*h*-HPCT and stained with the BM8 and ED2 antibodies. Representative photos are shown (c) for rat #5, whose blood *h*-Alb level increased continuously for up to 3 weeks and was > 15 ng/ml at 4 weeks, and (d) for rat #6, whose blood *h*-Alb level was continuously decreased until 3 weeks and was < 10 ng/ml at 4 weeks. The "P" and "C" labels in c and d indicate the portal and central vein regions, respectively. Scale bar = 100 μm.

were used for *h*-hepatocyte transplantation in the present study.

The suppression or deletion of the immunologic reactions of rats for xenotransplantation experiments has been achieved using a number of different methods, including lethal irradiation [6,16,17], an immunosuppressive agent [16], various antibodies [17], and splenectomization [16]. These immunosuppressed rats were utilized in studies of the transplantation of xenogeneic BMCs. Thus, the present study is the first to utilize immunosuppressed rats for the transplantation of xenogeneic tissue parenchymal cells, i.e., *h*-hepatocytes. The replacement rates achieved for xenogeneic BMCs in the previous studies were approximately 40% [17], 60% [6], and 85% [16]. Our conditioning regimen gives a replacement rate as high as 94%, although the number of transplanted *m*-BMCs in the present study is similar to those obtained in the previous studies. Presently, we cannot explain the higher replacement rate, as data on the survival of host BMCs and PBMCs are not available from the previous reports. However, in the present study, the irradiation regimen was more severe and the animals were much younger than that in the previous studies. These two differences may explain the higher replacement rate obtained in our study.

h-Hepatocytes were able to engraft the rat liver in our experimental conditions and proliferated to form small colonies. *h*-Alb was detectable in the blood samples from the hosts. These *h*-hepatocytes expressed several *h*-hepatocyte-specific mRNAs and proteins, which strongly suggests that these cells are able to maintain the original normal phenotypes in disconcordant xenogeneic environments. However, in contrast to SCID mice, the SCID rats did not allow ample proliferation of engrafted *h*-hepatocytes under the conditions that we adopted in the present study. There was no growth of *h*-hepatocyte colonies and no marked increase in blood *h*-Alb concentration, in spite of the high rate of replacement of m_{SCID}-BMCs. Some of the hosts showed small albeit steady increases in blood *h*-Alb levels up to 3 weeks post-*h*-HPCT, although the levels started to decrease at 4 weeks.

Our present data suggest a possible explanation for the low rate of repopulation of *h*-hepatocytes in SCID rats. Recently, it was demonstrated that

interspecies incompatibility of CD47 signaling in macrophages is related to immune responses following xenotransplantation, and the macrophages are activated through the interaction with xenogeneic cells in the liver [10,11]. We classified the chimeric SCID rats into two groups according to the blood level of *h*Alb, rats with *h*Alb > 15 ng/ml and those with *h*Alb < 10 ng/ml at 4 weeks post-*h*-HPCT. The *m*-macrophages were significantly enlarged in the former rats as compared with those in the latter rats. Taken together these facts, we speculate that these activated macrophages play a negative role (s) in the acceptance and proliferation of *h*-hepatocytes, i.e., the transplanted *h*-hepatocytes might be recognized and rejected by activated rat and/or mouse macrophages at 2–4 weeks post-*h*-HPCT. The possibility exists that the high concentration of uPA in the uPA/SCID mice negatively affects the normal functions of Kupffer cells, which permits *h*-hepatocytes to proliferate actively and to repopulate almost completely the host liver. Nevertheless, compared to transplantation into SCID mice, the engraftment rate of *h*-hepatocytes was extremely low in the SCID rats, which suggests a role for uPA in accelerating the engraftment of transplanted *h*-hepatocytes into the liver plate, for example, remodeling hepatic extracellular matrices.

The extent of the hepatic damage seen in the present study is also possibly related to the lower rate of *h*-hepatocyte repopulation. It is known that hepatocytes in the remnant live lobules show higher proliferation activities when the loss of liver volume is higher. We transplanted 2×10^5 *r*-hepatocytes from syngeneic wild-type [dipeptidyl peptidase-IV (DPPIV)$^+$] rats into the retrorsine-treated livers of both 40% PHx and 70% PHx mutant (DPPIV$^-$) rats and compared the repopulation rates of DPPIV$^+$-hepatocytes at 3 weeks post-*r*-HPCT in the 40% PHx and 70% PHx rats. We found that the liver repopulation rate for the 70% PHx rats was 10-fold higher than that for the 40% PHx rats (data not shown).

There are few studies that have transplanted *h*-hepatocytes into the liver of immunotolerant rats [18,19]. The researchers transplanted *h*-hepatocytes into the body cavities or thymus glands of embryonic and newborn rats to induce immunotolerance. Despite the fact that both the hosts and donors were quite young, the rate of hepatocyte engraftment was relatively low [18,19].

In the present study, we demonstrate for the first time that *h*-hepatocytes are capable of engrafting the rat liver and proliferating therein to form colonies. However, the *h*-hepatocytes did not show appreciable replication, as observed for liver-injured SCID mice. Further analyses of the *h*-hepatocyte-bearing SCID rats are necessary to reveal the immunologic mechanisms involved in xenogeneic transplantation, and to generate SCID rats with higher rates of *h*-hepatocyte repopulation.

Acknowledgements

We thank Ms. Y. Yoshizane, Ms. S. Nagai, and Ms. Y. Matsumoto for their excellent technical assistance, and all the members of the Yoshizato group at the Hiroshima Prefectural Institute of Industrial Science and Technology for advice and helpful discussions.

References

1. Lu C, Li AP. Species comparison in P450 induction: effects of dexamethasone, omeprazole, and rifampin on P450 isoforms 1A and 3A in primary cultured hepatocytes from man, Sprague-Dawley rat, minipig, and beagle dog. Chem Biol Interact 2001; 134: 271–281.
2. Guengerich FP. Comparisons of catalytic selectivity of cytochrome P450 subfamily enzymes from different species. Chem Biol Interact 1997; 106: 161–182.
3. Tateno C, Yoshizane Y, Saito N et al. Near completely humanized liver in mice shows human-type metabolic responses to drugs. Am J Pathol 2004; 165: 901–912.
4. Nishimura M, Yoshitsugu H, Yokoi T et al. Evaluation of mRNA expression of human drug-metabolizing enzymes and transporters in chimeric mouse with humanized liver. Xenobiotica 2005; 35: 877–890.
5. Tsuge M, Hiraga N, Takahashi H et al. Infection of human hepatocyte chimeric mouse with genetically engineered hepatitis B virus. Hepatology 2005; 42: 1046–1054.
6. Lubin I, Segall H, Erich P et al. Conversion of normal rats into SCID-like animals by means of bone marrow transplantation from SCID donors allows engraftment of human peripheral blood mononuclear cells. Transplantation 1995; 60: 740–747.
7. Seglen PO. Preparation of isolated rat liver cells. Methods Cell Biol 1976; 13: 29–83.
8. Yamasaki C, Tateno C, Aratani A et al. Growth and differentiation of colony-forming human hepatocytes in vitro. J Hepatol 2006; 44: 749–757.
9. Laconi E, Oren R, Mukhopadhyay DK et al. Long-term, near-total liver replacement by transplantation of isolated hepatocytes in rats treated with retrorsine. Am J Pathol 1998; 153: 319–329.
10. Ide K, Wang H, Tahara H et al. Role for CD47-SIRP-alpha signaling in xenograft rejection by macrophages. Proc Natl Acad Sci USA 2007; 104: 5062–5066.
11. Wang H, Verhalen J, Madariaga ML et al. Attenuation of phagocytosis of xenogeneic cells by manipulating CD47. Blood 2007; 109: 836–842.
12. Mercer DF, Schiller DE, Elliott JF et al. Hepatitis C virus replication in mice with chimeric human livers. Nat Med 2001; 7: 927–933.
13. Meuleman P, Libbrecht L, De Vos R et al. Morphological and biochemical characterization of a human liver in a uPA-SCID mouse chimera. Hepatology 2005; 41: 847–856.

14. Dandri M, Burda MR, Torok E et al. Repopulation of mouse liver with human hepatocytes and in vivo infection with hepatitis B virus. Hepatology 2001; 33: 981–988.
15. Azuma H, Paulk N, Ranade A et al. Robust expansion of human hepatocytes in $Fah^{-/-}/Rag2^{-/-}/Il\text{-}2rg^{-/-}$ mice. Nat Biotechnol 2007; 25: 903–910.
16. Miki T, Lee YH, Tandin A et al. Hamster-to-rat bone marrow xenotransplantation and humoral graft vs. host disease. Xenotransplantation 2001; 8: 213–221.
17. Nikolic B, Cooke DT, Zhao G et al. Both γδT cells and NK cells inhibit the engraftment of xenogeneic rat bone marrow cells and the induction of xenograft Tolerance in mice. J Immunol 2001; 166: 1398–1404.
18. Ouyang EC, Wu CH, Walton C et al. Transplantation of human hepatocytes into tolerized genetically immunocompetent rats. World J Gastroenterol 2001; 7: 324–330.
19. Wu CH, Ouyang EC, Walton C et al. Human hepatocytes transplanted into genetically immunocompetent rats are susceptible to infection by hepatitis B virus in situ. J Viral Hepat 2001; 8: 111–119.

ELSEVIER

Induction of Indoleamine 2,3-Dioxygenase in Livers Following Hepatectomy Prolongs Survival of Allogeneic Hepatocytes After Transplantation

Y.C. Lin, S. Goto, C. Tateno, T. Nakano, Y.F. Cheng, B. Jawan, Y.H. Kao, L.W. Hsu, C.Y. Lai, K. Yoshizato, and C.L. Chen

ABSTRACT

Objectives. Indoleamine 2,3-dioxygenase (IDO), which catalyzes the breakdown of tryptophan into kyneurenine, has immunologic significance for the induction of maternal tolerance and liver allograft tolerance by inhibiting T-cell activation. In the present study, we compared survival of syngeneic or allogeneic hepatocytes in livers with or without hepatectomy. Subsequently, we investigated gene expression and localization of IDO in the recipient liver.

Methods. DA and Fisher 344 rats were used in the following experimental groups: group 1, DA hepatocytes transplanted into hepatectomized Fisher 344 rats; group 2, Fisher 344 hepatocytes transplanted into hepatectomized Fisher 344 rats; group 3, DA hepatocytes transplanted into nonhepatectomized Fisher 344 rats; and group 4, Fisher 344 hepatocytes transplanted into nonhepatectomized Fisher 344 rats. After transplantation, the surviving cells were evaluated on day 5. The IDO signal of the recipient liver was detected by reverse transcriptase polymerase chain reaction (RT-PCR) and immunohistochemistry.

Results. In the hepatectomized groups subjected to allogeneic or syngeneic hepatocyte transplantation, the number of surviving hepatocytes was greater than in the nonhepatectomized group after transplantation. The IDO signals (RT-PCR) in the hepatectomized groups were stronger than those in the nonhepatectomized groups. Immunohistochemistry demonstrated that the IDO signal is located in liver antigen-presenting cells, such as Kupffer cells or dendritic cells, and not expressed in hepatocytes.

Conclusions. Our results demonstrated that IDO is induced in antigen-presenting cells of hepatectomized livers by which subsequently transplanted cells may be protected from rejection by inhibiting indirect or direct recognition of donor antigen and further T-cell activation.

ORTHOTOPIC LIVER TRANSPLANTATION is presently the only therapy that significantly improves the prognosis of liver disease. Unfortunately, the supply of livers available for transplantation is a small fraction of those needed. Transplantation of hepatocytes is a minimally invasive procedure that provides immediate metabolic sup-

From the Department of Surgery and Liver Transplantation Program (Y.C.L., S.G., T.N., Y.F.C., B.J., Y.H.K., L.W.H., C.Y.L.), Chang Gung Memorial Hospital, Kaohsiung Medical Center, Chang Gung University College of Medicine, Kaohsiung Hsien, Taiwan; the Hiroshima Prefecture Institute of Industrial Science and Technology (C.T., C.L.C), and the Department of Biological Science (K.Y.), Hiroshima University, Hiroshima, Japan.

Supported in part by grants from the National Science Council (NSC95-2314-B-182A-152) and Chang Gung Memorial Hospital (CMRPG850071) of Taiwan.

Address reprint requests to Chao-Long Chen, Liver Transplantation Program and Department of Surgery, Chang Gung Memorial Hospital, Kaohsiung Medical Center, Chang Gung University College of Medicine, 123 Ta-Pei Rd, Niao-Sung, Kaohsiung 833, Taiwan, R.O.C. E-mail: clchen@adm.cgmh.org.tw

0041-1345/08/$–see front matter
doi:10.1016/j.transproceed.2008.08.001

port until a donor liver becomes available for transplantation. In contrast to syngeneic hepatocytes, which can survive for long periods and even proliferate in recipients, allogeneic hepatocytes show massive apoptotic cell death due to acute rejection within 1 week after transplantation if not treated with immunosuppression.[1-3]

Indoleamine 2, 3-dioxygenase (IDO) is a cytosolic enzyme catalyzing the oxidative cleavage of the indole ring of l-tryptophan to *N*-formyl-kynurenine. Increasing evidence indicates that IDO suppresses T-cell responses by depleting local tryptophan, an essential amino acid for T-cell proliferation and function, and by the actions of the tryptophan metabolites, such as kyneurenine, which inhibit T-cell viability.[4] In the present study, we compared the survival of syngeneic or allogeneic hepatocytes in livers with or without hepatectomy. Subsequently, we investigated the gene expression and localization of IDO in livers after syngeneic or allogeneic hepatocyte transplantation with or without hepatectomy.

MATERIALS AND METHODS

In this experiment, DA and Fischer 344 rats with dipeptidyl peptidase IV (DPPIV) were used as the hepatocyte source for transplantation. Fischer 344 rats deficient in DPPIV were used as recipients. The experimental design included: group 1, DA hepatocytes (3×10^6) transplanted into 70% hepatectomized Fisher 344 rats (×3); group 2, Fisher 344 hepatocytes (3×10^6) transplanted to 70% hepatectomized Fisher 344 rats (×3); group 3, DA hepatocytes (10^7) transplanted into nonhepatectomized Fisher 344 rats (×3); and group 4, Fisher 344 hepatocytes (10^7) transplanted to nonhepatectomized Fisher 344 rats (×3). After transplantation, the rats were killed at day 5 to evaluate the surviving hepatocytes. Each lobe of the liver was collected in optimal cutting temperature medium or quick-frozen in liquid nitrogen for cryosection and RNA extraction. To calculate the surviving hepatocytes, we performed the DPPIV stain. In reverse transcriptase polymerase chain reaction (RT-PCR) analysis, c-DNA was synthesized by SuperScript-III first strand synthesis kit (Invitrogen, Carlsbad, Calif) and PCR performed using IDO, interferon (IFN)-γ and glyceraldehyde-3-phosphate dehydrogenase (GAPDH) primers. In immunohistochemistry, polyclonal antibodies against rat IDO (Santa Cruz Biotechnology, Santa Cruz, Calif) and monoclonal antibody ED2 to detect macrophages (BMA Biomedicals AG, Switzerland) were used to verify which cells expressed IDO in liver sections.

RESULTS

The surviving hepatocytes were observed in recipient liver sections by DPPIV staining. The numbers of surviving cells in each group were: group 1, 2.9 ± 1.6 cells/mm^2; group 2, 6.1 ± 2.7 cells/mm^2; group 3, 0 cells/mm^2; and group 4, 1.6 ± 1.4 cells/mm^2. RT-PCR analysis revealed that gene expression of both IDO and IFN-γ in the hepatectomized group was stronger than in the nonhepatectomized group (Fig 1). Immunohistochemical analysis demonstrated that IDO signals were located on liver antigen-presenting cells, such as Kupffer cells or dendritic cells, and not expressed in hepatocytes.

DISCUSSION

Recently, some experiments have demonstrated that transplantation of IDO overexpressing cells or organs showed significantly extended survival in recipients.[5,6] Our results also demonstrated that upregulation of IDO in antigen-presenting cells of hepatectomized livers was possibly induced by IFN-γ.[7] As a consequence, the transplanted cells may be protected from rejection by the upregulated IDO, which may directly or indirectly inhibit recognition of donor antigens and subsequent T-cell activation. Overexpression of IDO in the transplanted organ or tissue may act as a local

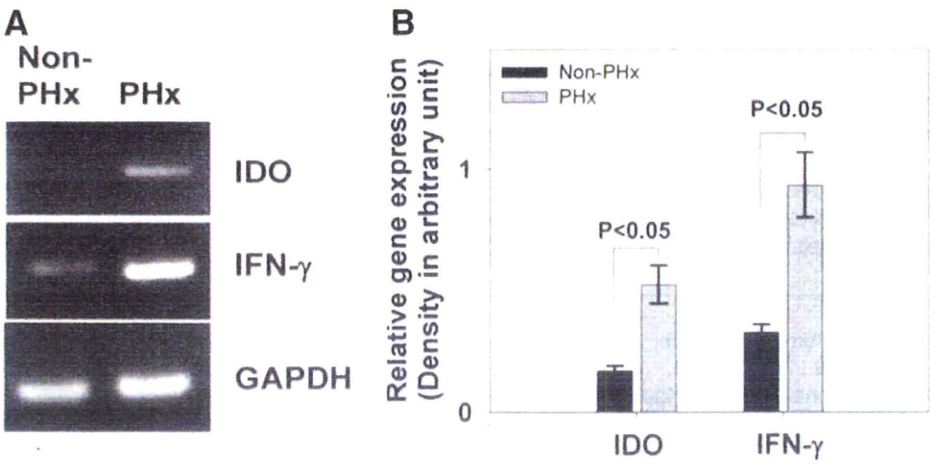

Fig 1. Gene expression of both IDO and IFN-γ are significantly upregulated in the partially hepatectomized (PHx) group compared with those in nonhepatectomized (Non-PHx) group. Rat liver tissues were collected from PHx and non-PHx groups 5 days after allogeneic (DA to Fisher 344) hepatocytes transplantation, followed by RNA extraction and RT-PCR analysis. **(A)** Electrophoresis of both IDO and IFN-γ. **(B)** Densitometric analysis indicates that gene expression of both IDO and IFN-γ in the PHx groups are significantly higher than those in the Non-PHx groups. The statistical analysis is performed using Student's *t*-test; $P < .05$ is considered significant.

immunosuppressive molecule to protect grafts from immune attack.

REFERENCES

1. Song E, Chen J, Min J, et al: FasL expression on splenocytes and its correlation with hepatocytic apoptosis during intrasplenically allogeneic hepatocyte transplantation. Asian J Surg 23:163, 2000

2. Strom SC, Chowdhury JR, Fox IJ: Hepatocyte transplantation for the treatment of human disease. Semin Liver Dis 19:39, 1999

3. Bumgardner GL, Orosz CG: Unusual patterns of alloimmunity evoked by allogeneic liver parenchymal cells. Immunol Rev 174:260, 2000

4. Moffett JR, Namboodiri MA: Tryptophan and the immune response. Immunol Cell Biol 81:247, 2003

5. Alexander AM, Crawford M, Bertera S, et al: Indoleamine 2,3-dioxygenase expression in transplanted NOD islets prolongs graft survival after adoptive transfer of diabetogenic splenocytes. Diabetes 51:356, 2002

6. Liu H, Liu L, Fletcher BS, et al: Novel action of indoleamine 2,3-dioxygenase attenuating acute lung allograft injury. Am J Respir Crit Care Med 173:566, 2006

7. Taylor MW, Feng GS: Relationship between interferon-gamma, indoleamine 2,3-dioxygenase, and tryptophan catabolism. FASEB J 11:2516, 1991

Journal of General Virology (2008), **89**, 2108–2113 DOI 10.1099/vir.0.83658-0

Establishment of an infectious genotype 1b hepatitis C virus clone in human hepatocyte chimeric mice

Takashi Kimura,[1,2] Michio Imamura,[1,2] Nobuhiko Hiraga,[1,2] Tsuyoshi Hatakeyama,[1,2] Daiki Miki,[1,2] Chiemi Noguchi,[1,2] Nami Mori,[1,2] Masataka Tsuge,[1,2] Shoichi Takahashi,[1,2] Yoshifumi Fujimoto,[1,2] Eiji Iwao,[3] Hidenori Ochi,[2,4] Hiromi Abe,[1,2,4] Toshiro Maekawa,[4] Keiko Arataki,[5] Chise Tateno,[2,6] Katsutoshi Yoshizato,[2,6] Takaji Wakita,[7] Toru Okamoto,[8] Yoshiharu Matsuura[8] and Kazuaki Chayama[1,2,4]

Correspondence
Kazuaki Chayama
chayama@hiroshima-u.ac.jp

[1]Department of Medicine and Molecular Science, Division of Frontier Medical Science, Programs for Biomedical Research, Graduate School of Biomedical Sciences, Hiroshima University, Hiroshima, Japan

[2]Liver Research Project Center, Hiroshima University, Hiroshima, Japan

[3]Research Division, Mitsubishi Tanabe Pharma Corporation, Osaka, Japan

[4]Laboratory for Liver Disease, SNP Research Center, Institute of Physical and Chemical Research (RIKEN), Yokohama, Japan

[5]Hirosimakinen-Hospital, Internal Medicine, Hiroshima, Japan

[6]Developmental Biology Laboratory, Department of Biological Science, Graduate School of Science, Hiroshima University, Higashihiroshima, Japan

[7]Department of Virology II, National Institute of Infectious Diseases, Shinjuku-ku, Japan

[8]Department of Molecular Virology, Research Institute for Microbial Diseases, Osaka University, Osaka, Japan

The establishment of clonal infection of hepatitis C virus (HCV) in a small-animal model is important for the analysis of HCV virology. A previous study developed models of molecularly cloned genotype 1a and 2a HCV infection using human hepatocyte-transplanted chimeric mice. This study developed a new model of molecularly cloned genotype 1b HCV infection. A full-length genotype 1b HCV genome, HCV-KT9, was cloned from a serum sample from a patient with severe acute hepatitis. The chimeric mice were inoculated intrahepatically with *in vitro*-transcribed HCV-KT9 RNA. Inoculated mice developed viraemia at 2 weeks post-infection, and this persisted for more than 6 weeks. Passage experiments indicated that the sera of these mice contained infectious HCV. Interestingly, a similar clone, HCV-KT1, in which the poly(U/UC) tract was 29 nt shorter than in HCV-KT9, showed poorer *in vivo* infectivity and replication ability. An *in vitro* study showed that no virus was produced in the culture medium from HCV-KT9-transfected cells. In conclusion, this study developed a genetically engineered genotype 1b HCV-infected mouse. This mouse model will be useful for the study of HCV virology, particularly the mechanism underlying the variable resistance of HCV genotypes to interferon therapy.

Received 13 December 2007
Accepted 14 May 2008

INTRODUCTION

Hepatitis C virus (HCV), a positive-sense, single-stranded RNA virus, infects and replicates efficiently only in the hepatocytes of humans and chimpanzees. There are many genotypes of HCV distributed worldwide (Simmonds *et al.*, 1993); among them genotype 1b is the major genotype in Asia, including Japan, and is known to be one of the most resistant genotypes to interferon (IFN) therapy (Fried *et al.*, 2002). Until recently, studies of HCV replication have long been hampered by the lack of a virus culture system. The development of HCV replicon systems has allowed the

The GenBank/EMBL/DDBJ accession numbers for the sequences of HCV-KT9 and HCV-KT1 determined in this work are AB435162 and AB426117, respectively.

study of the mechanisms of replication of HCV (Lohmann *et al.*, 1999). However, these replicons lack structural proteins, do not replicate efficiently without adaptive mutations and do not produce infectious virions. Recently, it was reported that the genotype 2a full-length JFH-1 genome replicated efficiently in Huh7 cells without adaptive mutations and produced virions that were infectious for both naïve cells and chimpanzees, as well as for a human hepatocyte-transplanted chimeric mouse (Wakita *et al.*, 2005; Zhong *et al.*, 2005; Lindenbach *et al.*, 2006). To date, five full-length genotype 1b clones, HCV-N (Beard *et al.*, 1999), Con-1 (Bukh *et al.*, 2002), HCV-J4 (Okamoto *et al.*, 1992), HCV-CG1b (Thomson *et al.*, 2001) and HCV-BK (Takamizawa *et al.*, 1991), have been demonstrated to be infectious by intrahepatic inoculation of transcribed HCV RNA into the liver of chimpanzees. Among these, only the HCV-CG1b genome is reported to produce HCV particles when transfected into Huh7 cells (Heller *et al.*, 2005).

Although the chimpanzee is a useful animal model for the study of HCV infection, there are ethical restrictions on the use of this animal. Instead, Mercer *et al.* (2001) developed a useful small-animal model for the study of HCV infection using chimeric urokinase-type plasminogen activator (uPA)/severe combined immunodeficiency (SCID) mice (which are immunodeficient and undergo liver failure) with engrafted human hepatocytes. This HCV-infected mouse model is reported to be useful for evaluating anti-HCV drugs such as IFN-α and anti-NS3 protease (Kneteman *et al.*, 2006). We have previously described methods to improve the replacement levels of human hepatocytes in this mouse model (Tateno *et al.*, 2004) and we have developed a reverse genetics system for hepatitis B virus (Tsuge *et al.*, 2005) and HCV (Hiraga *et al.*, 2007). In the present study, we report the establishment of an infectious genotype 1b HCV clone that infects and replicates efficiently in human hepatocyte chimeric mice.

METHODS

Cloning of infectious genotype 1b HCV isolate. Serum samples were obtained from a 43-year-old physician who developed severe acute hepatitis after needle stick exposure from a patient with chronic hepatitis C. On admission, the serum total bilirubin concentration was 10.0 mg dl^{-1} and the prothrombin time was 40 %. The patient tested positive for HCV antibodies by a third-generation radioimmunoassay (Ortho-Clinical Diagnostics) and for HCV RNA by RT-PCR. Serum HCV RNA was quantified using an Amplicor Monitor HCV test (Roche Diagnostics). The HCV RNA titre was 2.5×10^6 copies ml^{-1} on admission and then decreased gradually. Fig. 1 shows the serial changes in alanine aminotransferase (ALT) as a measure of liver function and HCV RNA levels in this patient. Serum samples obtained in the early phase of infection were used for cloning the full-length genome.

RNA extraction, cDNA synthesis, plasmid construction and RNA transcription. Total RNA was extracted from 100 µl serum samples using SepaGene RV-R (Sanko Junyaku) and reverse transcribed with random hexamers and ReverTra Ace reverse transcriptase (Toyobo) according to the manufacturer's instructions. PCR primers were designed based on the sequence of HCV-Con1 (GenBank accession no. AJ238799; Bukh *et al.*, 2002). Five overlapping cDNA segments (nt 1–2292, 2269–6715, 6696–9094, 7564–9404 and 9361–9605; nucleotide numbers are those of HCV-Con1) were amplified by PCR with TaKaRa LA *Taq* polymerase (Takara Biochemicals) using the above cDNA. Amplified products were separated by agarose gel electrophoresis. Nucleotide sequences were determined using a Big Dye Terminator Mix Cycle Sequencing kit (Applied Biosystems Japan) with an automated DNA sequencer (model 310; PE Biosystems). We corrected the nucleotide sequences of the obtained clones by site-directed mutagenesis and made them identical to the nucleotide sequences obtained by direct sequencing. Naturally occurring restriction enzyme cutting sites were utilized to clone each segment. We utilized the vector pBR322 and created a multiple-cloning site under the control of the T7 promoter by ligating a linker at restriction enzyme cutting sites as they appeared in order from 5′ to 3′ in the HCV sequences (Fig. 2a). Each segment of HCV was cloned into this vector to generate the full-length clones. The HCV-KT9 clone was established using the 3′-terminal fragment with the longest poly(U/UC) tract length (115 nt), which should have a high replication ability (Friebe & Bartenschlager, 2002; Yi & Lemon, 2003; You & Rice, 2008). A clone with a shorter poly(U/UC) tract length (86 nt), HCV-KT1, was also generated. A polymerase-deficient mutant with an amino acid substitution in the GDD motif (GDD→GND; HCV-KT9-GND) was generated using a Quick Change Site-Directed Mutagenesis kit (Stratagene). After digesting the plasmid with *Xba*I (New England BioLabs) at the 3′ end of the HCV cDNA, HCV RNA was transcribed using T7 RNA polymerase (MEGAscript; Ambion) at 37 °C for 3 h in a 100 µl reaction mixture, according to the manufacturer's instructions. The RNA was analysed using denaturing agarose gel electrophoresis and kept at −80 °C until use.

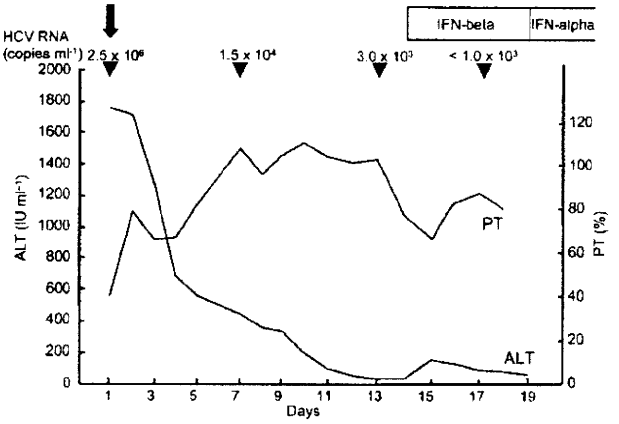

Fig. 1. Clinical course of a patient with severe acute hepatitis C. Alanine aminotransferase (ALT) and prothrombin time (PT) are shown from the day of admission (day 1). The patient was treated daily with 10^6 U IFN-β intravenously for 5 days, followed by 10^6 U IFN-α intramuscularly three times a week for 6 months. HCV RNA was measured on days 1, 7, 13 and 17 (arrowheads). A serum sample was taken on day 1 (arrow) and used to clone the full-length HCV genome.

Construction of a phylogenetic tree. A phylogenetic tree was constructed based on the entire nucleotide sequences of 26 full-length genotype 1b clones plus HCV-KT9. The total number of synonymous and non-synonymous substitutions among the nucleotide sequences was estimated using the method of Gojobori *et al.* (1982) and a phylogenetic tree was constructed by the neighbour-joining method (Saitou & Nei, 1987).

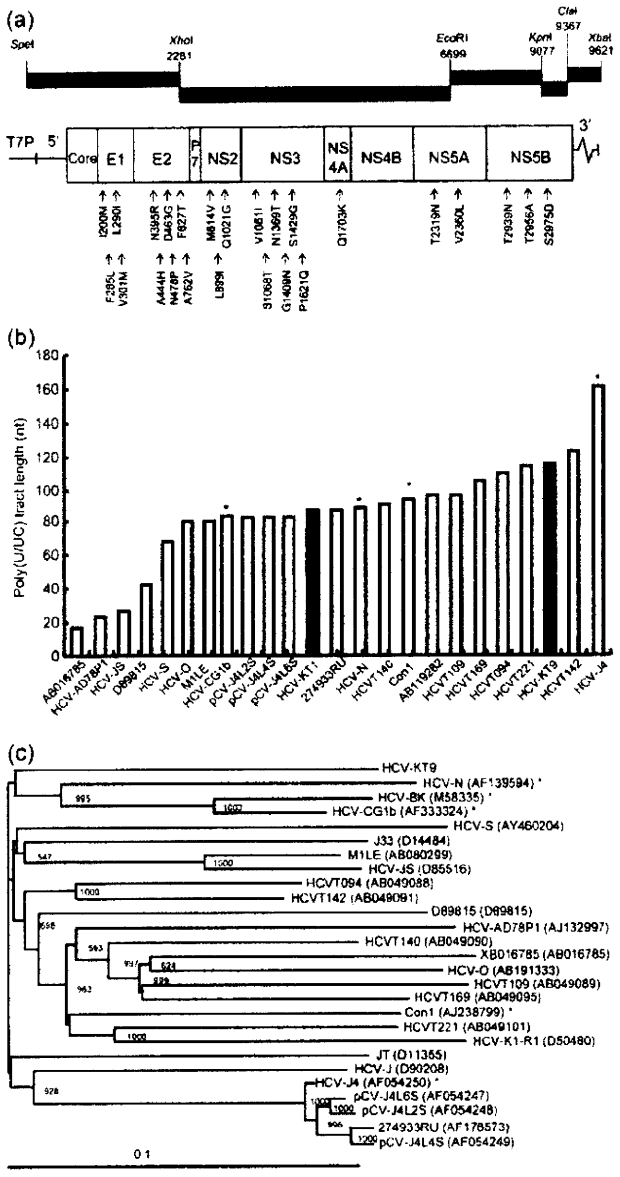

Fig. 2. (a) Schematic diagram of the organization of the cDNA clone HCV-TK9. The T7 RNA promoter (T7P) is located immediately upstream of the HCV genome. Restriction enzyme sites that were used to create clone HCV-KT9 are labelled according to their nucleotide position within the HCV sequence. Amino acid sequences unique to HCV-KT9 compared with 26 other HCV genotype 1b isolates are indicated at the bottom of the figure, with the position of the repaired amino acid residues noted within the polyprotein. (b) Length of the poly(U/UC) tracts of HCV-KT1, HCV-KT9 and 22 other HCV genotype 1b clones reported previously. Asterisks indicate clones confirmed to be infectious by experiments using chimpanzees. (c) Phylogenetic tree constructed with HCV-KT9 and 26 genotype 1b HCV whole-genome sequences. Bar, number of nucleotide substitutions per site. Asterisks indicate clones confirmed to be infectious in experiments using chimpanzees.

Intrahepatic injection experiments in human hepatocyte chimeric mice. We used methods described previously (Tateno *et al.*, 2004) to generate uPA$^{+/+}$/SCID$^{+/+}$ mice and transplant human hepatocytes. All mice used in this study were transplanted with frozen human hepatocytes obtained from the same donor. Mouse serum concentrations of human serum albumin (HSA) correlate with the repopulation index and were measured as described previously (Tateno *et al.*, 2004). Intrahepatic injection of RNA, extraction of serum samples and euthanasia were performed under ether anaesthesia. Briefly, 500 µl RNA solution containing 30 µg transcribed HCV RNA was injected into the liver of anaesthetized chimeric mice through a small abdominal incision. RNA extraction from mouse serum samples, quantification of HCV RNA and nested PCR were performed as described previously (Hiraga *et al.*, 2007). All animal protocols described in this study were performed in accordance with the guidelines of the local committee for animal experiments and under the approval of the Ethics Review Committee for Animal Experimentation of the Graduate School of Biomedical Sciences, Hiroshima University.

Cell culture, RNA transfection and measurement of HCV core antigen. The human hepatoma cell line Huh7 was maintained in Dulbecco's modified Eagle's medium (Sigma) containing 10% fetal calf serum. RNA transfection and measurement of HCV core antigen in the culture medium were performed as described previously (Wakita *et al.*, 2005).

Statistical analysis. The infectious ratio of chimeric mice was compared and the differences assessed using a χ^2 test. Differences in HCV RNA replication ability *in vitro* were analysed statistically by one-way analysis of variance followed by Scheffe's test. A P value of less than 0.05 was considered statistically significant.

RESULTS

Characteristics of genotype 1b clones HCV-KT9 and HCV-KT1

The entire genome of HCV cDNA was assembled from five DNA fragments (Fig. 2a). We obtained 24 3′-extremity clones with different poly(U/UC) tract lengths. We selected the clone with the longest (U/UC) tract because a previous study indicated that the length of poly(U/UC) tract correlates with HCV replication in an HCV replicon system (Friebe & Bartenschlager, 2002; Yi & Lemon, 2003; You & Rice, 2008). The length of the poly(U/UC) tract in the longest 3′ clone was 115 nt. The entire genome length of the HCV-KT9 clone using this longest 3′ clone was 9621 nt. We also generated the clone HCV-KT1 with a shorter (86 nt) poly (U/UC) tract to compare the replication abilities of these clones. The lengths of the poly(U/UC) tracts of 22 clones deposited in GenBank are shown in Fig. 2(b). All infectious clones had a poly(U/UC) tract longer than 80 nt. Fig. 2(c) shows a phylogenetic tree constructed using the nucleotide sequences of the 26 full-length genotype 1b clones published to date. Interestingly, the sequence of HCV-KT9 was closest to that of HCV-CG1b (GenBank accession no. AF333324), which has been reported to be infectious, and formed a cluster with two other infectious clones, HCV-N (Beard *et al.*, 1999) and HCV-BK (Takamizawa *et al.*, 1991). We compared the amino acid

sequences of HCV-KT9 with an alignment of the sequences of the 26 other genotype 1b strains. All HCV full-length clones reported from Japan were included in these 26 strains. Based on these comparisons, we identified 25 aa unique to HCV-KT9 (Fig. 2a). We found that the amino acid sequence of the IFN sensitivity-determining region in the NS5A region, which has been suggested to mediate IFN resistance via interaction with the cellular protein kinase R (Enomoto *et al.*, 1996; Gale *et al.*, 1997), was that of the wild-type.

Intrahepatic injection of HCV-KT1 and HCV-KT9 RNAs into human hepatocyte chimeric mice

In the next experiments, 30 μg *in vitro*-transcribed RNA of HCV-KT1, HCV-KT9 or HCV-KT9-GND was injected into the livers of chimeric mice. Eight of 10 (80%) HCV-KT9-injected mice developed measurable viraemia at 2 weeks post-inoculation (Table 1 and Fig. 3), with the HCV RNA titre reaching 1.1×10^6 to 8.8×10^6 copies ml^{-1} at 6 weeks post-inoculation (Fig. 3). To check for the presence of infectious HCV in the serum of HCV-KT9-infected mice, each of five naïve mice was injected with 10 μl serum sample (containing 3.5×10^5 copies of HCV) obtained from an HCV-KT9-infected mouse 6 weeks after inoculation. All five naïve mice became positive for HCV RNA, as confirmed by nested PCR, at 2 weeks post-inoculation and two mice developed persistent viraemia (Fig. 4). These results indicated that the serum of HCV-KT9-injected mice contained infectious HCV. In contrast to HCV-KT9, none of the three mice injected with HCV-KT9-GND RNA developed viraemia (Table 1). These results indicated that HCV-KT9 replicates efficiently in mice livers and produces infectious virus continuously. On the other hand, only one out of seven HCV-KT1-injected mice (14%) developed measurable viraemia (Table 1 and Fig. 3). The level of viraemia was low in this HCV-KT1-infected mouse, HCV RNA was negative by nested PCR at 2 weeks after inoculation and the titre was only 2.2×10^4 copies ml^{-1} at 4 weeks post-inoculation (Fig. 3). These results confirmed the importance of the poly(U/UC) tract length in experimentally induced viraemia.

The nucleotide and amino acid sequences of the viral genome isolated from an HCV-KT9-injected mouse (Fig. 3) at 6 weeks after RNA injection were identical to the injected HCV-KT9 (data not shown). We tried to reclone the poly(U/UC) tract in the HCV-KT1-infected mouse, but it was impossible to reamplify the HCV cDNA using the remaining small amount of serum.

Table 1. Correlation between length of the poly(U/UC) tract and HCV infection

Clone	Length of poly(U/UC) tract	Number of mice			Infection ratio
		Infected	Not infected	Total	
HCV-KT1	86	1	6	7	14%
HCV-KT9	115	8	2	10	80%*
HCV-KT9-GND	115	0	3	3	0%

*P=0.015, compared with HCV-KT1.

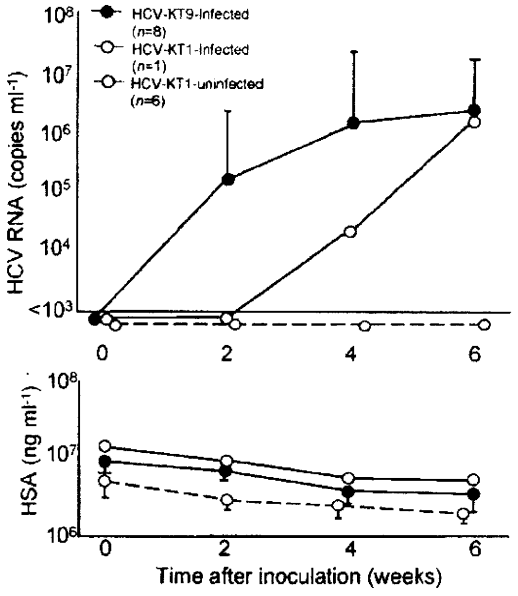

Fig. 3. Changes in HCV RNA levels and HSA concentrations in the sera of mice infected with clonal HCV. Mice were inoculated intrahepatically with 30 μg *in vitro*-transcribed HCV RNA. Eight of the ten HCV-KT9-infected mice (80%), one of the seven HCV-KT1-infected mice (14%) and none of the three HCV-KT9-GND-infected mice became positive for HCV RNA. The results for six HCV-KT1-uninfected mice are also shown. Mice serum samples were obtained every 2 weeks post-infection for analysis of HCV RNA titres. Data are shown as mean ± SD.

Analysis of virus production from HCV-KT9-transfected cells

Next, we evaluated the ability of the HCV-KT9 clone to replicate in transfected Huh7 cells. In these experiments, we used JFH-1 RNA, which is known to replicate efficiently in cell cultures, as control (Wakita *et al.*, 2005). Core protein was secreted efficiently from JFH-1 RNA-transfected Huh7 cells. In contrast, we did not observe any measurable levels of core protein in the supernatant of HCV-KT9-transfected cells (Fig. 5), suggesting a minimal replication ability of HCV-KT9 to produce and release virus into the supernatant.

DISCUSSION

In this study, we described the establishment of a genotype 1b clone, HCV-KT9, that replicated efficiently following injection of the transcribed RNA into chimeric mouse liver.

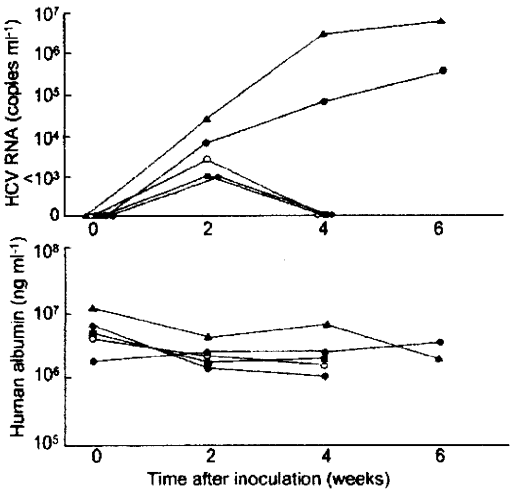

Fig. 4. Passage experiments of HCV in naïve chimeric mice. Five naïve chimeric mice were inoculated intravenously with 10 µl serum sample (containing 3.5×10^5 copies HCV) obtained from an HCV-KT9-infected mouse at week 6 post-inoculation. Serum samples were obtained at the indicated time intervals for the measurement of HCV RNA levels and HSA concentrations. Data represent the changes in five individual mice.

The key factor that determines the infectivity of HCV clones has not yet been established. We previously established a clone from HCV that replicated in a chimeric mouse after injection of serum from a chronically HCV-infected patient. However, we did not observe viraemia after intrahepatic injection of the transcribed RNA from this clone (unpublished results). In contrast, injection of HCV-KT9 RNA in the present study resulted in viraemia in eight out of ten mice (80 %). The fact that the nucleotide and amino acid sequences of the virus recovered from the infected mice were identical to those of the HCV-KT9 clone indicated that no adaptive mutation was necessary for this clone to replicate in the chimeric mouse.

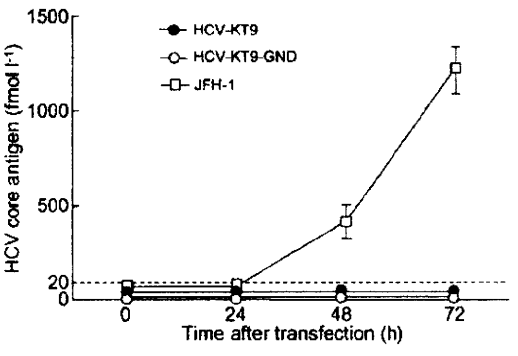

Fig. 5. Time-course studies of HCV core protein secretion into the culture medium of HCV RNA-transfected cells. Huh7 cells were transfected with 10 µg HCV-KT9, HCV-KT9-GND or JFH-1 RNA. HCV core antigen in the culture medium was measured at 24, 48 and 72 h after transfection. Data are shown as mean ± SD of HCV core protein levels obtained from three independent transfection experiments.

Interestingly, the clone was obtained from a patient with severe acute hepatitis. This is similar to JFH-1, an HCV clone with a strong replication ability in cultured cell lines, chimpanzees and chimeric mice, which was cloned from serum samples of a patient who developed acute fulminant hepatitis with a high virus titre (Wakita *et al.*, 2005). A virus that replicates in the early stage of infection may have strong replication ability, which may be lost in the chronic phase of infection.

A key amino acid substitution may be present in one (or some) of the amino acids unique to this clone (Fig. 2a). We also showed that clone HCV-KT1, which differs from HCV-KT9 only in the length of the poly(U/UC) tract, had a poorer replication ability in mice (Table 1 and Fig. 3). However, there is a possibility that a shorter poly(U/UC) tract only slows down the rate of infection, as the HCV RNA titre in the HCV-KT1-infected mouse at 6 weeks after inoculation was similar to that in HCV-KT9-infected mice (Fig. 3). It has been reported that the length and composition of the poly(U/UC) tract is important for the replication of HCV replicons (Friebe & Bartenschlager, 2002; Yi & Lemon, 2003; You & Rice, 2008). However, no replication advantage of a poly(U/UC) tract longer than 86 bp was revealed in this study. This may be due to differences *in vitro* and *in vivo*, where the innate immune response against the virus may be more robust than in cell culture.

As shown in the present study, reverse genetics of HCV has become available for studies of HCV replication. The important factors for virus replication suggested above can be analysed further using this system.

We also examined the response of HCV-KT9-infected mice to IFN treatment. Three HCV-KT9-infected mice were treated with daily intramuscular injections of 1000 IU IFN-α (g body weight)$^{-1}$ for 2 weeks. This regimen resulted in a reduction in HCV RNA levels of only 1.0 log copies ml^{-1} (data not shown). These results are consistent with our previous study, which showed a similar low-level reduction in HCV RNA in mice infected with a genotype 1a clone, and differ from our previous results in mice infected with HCV genotype 2a, which became negative for HCV RNA following daily treatment with 1000 IU IFN-α (g body weight)$^{-1}$ for 2 weeks (Hiraga *et al.*, 2007). These results are in agreement with our clinical experience that genotype 1 is more resistant to IFN therapy than genotype 2. As shown in the present study and previously (Hiraga *et al.*, 2007), reverse genetics of HCV with three genotypes, 1a, 1b and 2a, is now available. By recombination of these clones or the establishment of mutants with nucleotide and amino acid sequences similar to each other, it may be possible to clarify the mechanism underlying the variability in susceptibility of HCV genotypes to IFN.

In this study, HCV-KT9 showed no virus production ability *in vitro*. Recently, Kato *et al.* (2007) reported that the genotype 1b HCV clone CG1b replicated in Huh7.5.1 cells and produced infectious HCV. It will be of interest to create chimeric viruses of HCV-KT9 and HCV-CG1b, and to determine the mutations that are important for virus production *in vitro*.

In summary, we established an infection model of a genotype 1b HCV clone using human hepatocyte chimeric mice. This model will be useful for studies of HCV replication, particularly the mechanism underlying the variable resistance of HCV genotypes to IFN therapy.

ACKNOWLEDGEMENTS

The authors thank Rie Akiyama and Kana Kunihiro for their technical help and Dr Francis V. Chisari for providing the Huh7.5.1 cells. This work was supported in part by Grants-in-Aid for scientific research and development from the Ministry of Education, Sports, Culture and Technology and the Ministry of Health, Labor and Welfare, Japan.

REFERENCES

Beard, M. R., Abell, G., Honda, M., Carroll, A., Gartland, M., Clarke, B., Suzuki, K., Lanford, R., Sangar, D. V. & Lemon, S. M. (1999). An infectious molecular clone of a Japanese genotype 1b hepatitis C virus. *Hepatology* **30**, 316–324.

Bukh, J., Pietschmann, T., Lohmann, V., Krieger, N., Faulk, K., Engle, R. E., Govindarajan, S., Shapiro, M., St Claire, M. & other authors (2002). Mutations that permit efficient replication of hepatitis C virus RNA in Huh-7 cells prevent productive replication in chimpanzees. *Proc Natl Acad Sci U S A* **99**, 14416–14421.

Enomoto, N., Sakuma, I., Asahina, Y., Kurosaki, M., Murakami, T., Yamamoto, C., Ogura, Y., Izumi, N., Marumo, F. & other authors (1996). Mutations in the nonstructural protein 5A gene and response to interferon in patients with chronic hepatitis C virus 1b infection. *N Engl J Med* **334**, 77–81.

Friebe, P. & Bartenschlager, R. (2002). Genetic analysis of sequences in the 3′ nontranslated region of hepatitis C virus that are important for RNA replication. *J Virol* **76**, 5326–5338.

Fried, M. W., Shiffman, M. L., Reddy, K. R., Smith, C., Marinos, G., Goncales, F. L., Jr, Haussinger, D., Diago, M., Carosi, G. & other authors (2002). Peginterferon alfa-2a plus ribavirin for chronic hepatitis C virus infection. *N Engl J Med* **347**, 975–982.

Gale, M. J., Jr, Korth, M. J., Tang, N. M., Tan, S. L., Hopkins, D. A., Dever, T. E., Polyak, S. J., Gretch, D. R. & Katze, M. G. (1997). Evidence that hepatitis C virus resistance to interferon is mediated through repression of the PKR protein kinase by the nonstructural 5A protein. *Virology* **230**, 217–227.

Gojobori, T., Ishii, K. & Nei, M. (1982). Estimation of average number of nucleotide substitutions when the rate of substitution varies with nucleotide. *J Mol Evol* **18**, 414–423.

Heller, T., Saito, S., Auerbach, J., Williams, T., Moreen, T. R., Jazwinski, A., Cruz, B., Jeurkar, N., Sapp, R. & other authors (2005). An in vitro model of hepatitis C virion production. *Proc Natl Acad Sci U S A* **102**, 2579–2583.

Hiraga, N., Imamura, M., Tsuge, M., Noguchi, C., Takahashi, S., Iwao, E., Fujimoto, Y., Abe, H., Maekawa, T. & other authors (2007). Infection of human hepatocyte chimeric mouse with genetically engineered hepatitis C virus and its susceptibility to interferon. *FEBS Lett* **581**, 1983–1987.

Kato, T., Matsumura, T., Heller, T., Saito, S., Sapp, R. K., Murthy, K., Wakita, T. & Liang, T. J. (2007). Production of infectious hepatitis C virus of various genotypes in cell cultures. *J Virol* **81**, 4405–4411.

Kneteman, N. M., Weiner, A. J., O'Connell, J., Collett, M., Gao, T., Aukerman, L., Kovelsky, R., Ni, Z. J., Zhu, Q. & other authors (2006). Anti-HCV therapies in chimeric scid-Alb/uPA mice parallel outcomes in human clinical application. *Hepatology* **43**, 1346–1353.

Lindenbach, B. D., Meuleman, P., Ploss, A., Vanwolleghem, T., Syder, A. J., McKeating, J. A., Lanford, R. E., Feinstone, S. M., Major, M. E. & other authors (2006). Cell culture-grown hepatitis C virus is infectious in vivo and can be recultured in vitro. *Proc Natl Acad Sci U S A* **103**, 3805–3809.

Lohmann, V., Korner, F., Koch, J., Herian, U., Theilmann, L. & Bartenschlager, R. (1999). Replication of subgenomic hepatitis C virus RNAs in a hepatoma cell line. *Science* **285**, 110–113.

Mercer, D. F., Schiller, D. E., Elliott, J. F., Douglas, D. N., Hao, C., Rinfret, A., Addison, W. R., Fischer, K. P., Churchill, T. A. & other authors (2001). Hepatitis C virus replication in mice with chimeric human livers. *Nat Med* **7**, 927–933.

Okamoto, H., Kojima, M., Okada, S., Yoshizawa, H., Iizuka, H., Tanaka, T., Muchmore, E. E., Peterson, D. A., Ito, Y. & other authors (1992). Genetic drift of hepatitis C virus during an 8.2-year infection in a chimpanzee: variability and stability. *Virology* **190**, 894–899.

Saitou, N. & Nei, M. (1987). The neighbor-joining method: a new method for reconstructing phylogenetic trees. *Mol Biol Evol* **4**, 406–425.

Simmonds, P., Holmes, E. C., Cha, T. A., Chan, S. W., McOmish, F., Irvine, B., Beall, E., Yap, P. L., Kolberg, J. & other authors (1993). Classification of hepatitis C virus into six major genotypes and a series of subtypes by phylogenetic analysis of the NS-5 region. *J Gen Virol* **74**, 2391–2399.

Takamizawa, A., Mori, C., Fuke, I., Manabe, S., Murakami, S., Fujita, J., Onishi, E., Andoh, T., Yoshida, I. & other authors (1991). Structure and organization of the hepatitis C virus genome isolated from human carriers. *J Virol* **65**, 1105–1113.

Tateno, C., Yoshizane, Y., Saito, N., Kataoka, M., Utoh, R., Yamasaki, C., Tachibana, A., Soeno, Y., Asahina, K. & other authors (2004). Near completely humanized liver in mice shows human-type metabolic responses to drugs. *Am J Pathol* **165**, 901–912.

Thomson, M., Nascimbeni, M., Gonzales, S., Murthy, K. K., Rehermann, B. & Liang, T. J. (2001). Emergence of a distinct pattern of viral mutations in chimpanzees infected with a homogeneous inoculum of hepatitis C virus. *Gastroenterology* **121**, 1226–1233.

Tsuge, M., Hiraga, N., Takaishi, H., Noguchi, C., Oga, H., Imamura, M., Takahashi, S., Iwao, E., Fujimoto, Y. & other authors (2005). Infection of human hepatocyte chimeric mouse with genetically engineered hepatitis B virus. *Hepatology* **42**, 1046–1054.

Wakita, T., Pietschmann, T., Kato, T., Date, T., Miyamoto, M., Zhao, Z., Murthy, K., Habermann, A., Krausslich, H. G. & other authors (2005). Production of infectious hepatitis C virus in tissue culture from a cloned viral genome. *Nat Med* **11**, 791–796.

Yi, M. & Lemon, S. M. (2003). 3′ Nontranslated RNA signals required for replication of hepatitis C virus RNA. *J Virol* **77**, 3557–3568.

You, S. & Rice, C. M. (2008). 3′ RNA elements in hepatitis C virus replication: kissing partners and long poly(U). *J Virol* **82**, 184–195.

Zhong, J., Gastaminza, P., Cheng, G., Kapadia, S., Kato, T., Burton, D. R., Wieland, S. F., Uprichard, S. L., Wakita, T. & other authors (2005). Robust hepatitis C virus infection *in vitro*. *Proc Natl Acad Sci U S A* **102**, 9294–9299.

Toxicologic Pathology

http://tpx.sagepub.com

Human Hepatocytes Can Repopulate Mouse Liver: Histopathology of the Liver in Human Hepatocyte-Transplanted Chimeric Mice and Toxicologic Responses to Acetaminophen

Yasushi Sato, Hiroshi Yamada, Kazuhide Iwasaki, Chise Tateno, Tsuyoshi Yokoi, Katsutoshi Yoshizato and Ikuo Horii

Toxicol Pathol 2008; 36; 581 originally published online May 8, 2008;
DOI: 10.1177/0192623308318212

The online version of this article can be found at:
http://tpx.sagepub.com/cgi/content/abstract/36/4/581

Published by:
SAGE
http://www.sagepublications.com

On behalf of:

Society of Toxicologic Pathology

Toxicologic Pathology, 36: 581-591, 2008

ISSN: 0192-6233 print / 1533-1601 online
DOI: 10.1177/0192623308318212

Human Hepatocytes Can Repopulate Mouse Liver: Histopathology of the Liver in Human Hepatocyte-Transplanted Chimeric Mice and Toxicologic Responses to Acetaminophen

YASUSHI SATO,[1] HIROSHI YAMADA,[1] KAZUHIDE IWASAKI,[2] CHISE TATENO,[3] TSUYOSHI YOKOI,[4] KATSUTOSHI YOSHIZATO,[3,5] AND IKUO HORII[1]

[1]*Drug Safety Research & Development, Pfizer Global Research & Development, Nagoya Laboratories, 5-2 Taketoyo, Chita-gun, Aichi, Japan*
[2]*Pharmacokinetics Dynamics Metabolism, Pfizer Global Research & Development, Nagoya Laboratories, 5-2 Taketoyo, Chita-gun, Aichi, Japan*
[3]*Yoshizato Project, Hiroshima Prefectural Institute of Industrial Science and Technology, Cooperative Link of Unique Science and Technology for Economy Revitalization,* 1-3-2 Kagamiyama, *Higashi-Hiroshima City, Hiroshima, Japan*
[4]*Faculty of Pharmaceutical Sciences, Kanazawa University,* Kakuma-machi, Kanazawa, Japan
[5]*Department of Biological Science, Graduate School of Science, Hiroshima, University, 1-3-2 Kagamiyama, Higashi-Hiroshima City, Hiroshima, Japan*

ABSTRACT

A human hepatocyte-transplanted chimeric mouse has been established by transplantation of human hepatocytes to urokinase-type plasminogen activator transgenic/severe combined immunodeficiency (uPA$^{+/+}$/SCID) mice. These chimeric mice have various amounts of human hepatocytes that proliferate extensively and progressively replace mouse hepatocytes. In the chimeric liver, hepatic cords and sinusoid-like structures were observed. The human hepatocytes expressed human albumin, human cytochrome P450 enzymes, and human transporter proteins. Furthermore, electron microscopic analysis demonstrated bile canaliculi associated with human hepatocytes in the chimeric mouse livers. These results indicate that the chimeric mouse livers contain functionally intact and differentiated human hepatocytes. Additionally, the toxicologic response of hepatocytes to acetaminophen (APAP) administration was compared in normal and chimeric mouse livers. Following 1,400 mg/kg APAP, mild hepatocellular degeneration was observed in the human hepatocyte areas in the chimeric mice, compared with severe centrilobular hepatocellular necrosis in the ICR mouse livers. In conclusion, these chimeric livers contain functionally differentiated human hepatocytes, and are less susceptible to APAP toxicity, compared to ICR mice.

Keywords: chimeric mouse; humanized liver; human hepatocyte; bile canaliculi; cytochrome P450; multidrug resistance protein; acetaminophen.

INTRODUCTION

The main functions of the liver include metabolism of nutrients, synthesis and secretion of bile, synthesis of the plasma proteins, destruction of spent blood cells, and detoxification of metabolic waste products and various toxins. Owing to the functional diversity and highly developed three-dimensional architectures of hepatocytes, vasculature, and associated nonparenchymal cells, investigations of human liver functions have been limited to in vitro and ex vivo assays.

Recently, a human hepatocyte chimeric mouse was established by transplantation of human hepatocytes into the liver of homozygous urokinase-type plasminogen activator transgenic/severe combined immunodeficiency (uPA$^{+/+}$/SCID) mice (Tateno et al., 2004). Heterozygous uPA-transgenic mice (albumin promotor) were crossed with SCID mice to produce uPA$^{+/-}$/SCID mice that were then crossed to produce uPA$^{+/+}$/SCID mice. The uPA$^{+/+}$/SCID mouse undergoes continuous hepatocellular damage due to expression of the albumin-uPA transgene (Tateno et al., 2004), and also has immunologic tolerance to human hepatocytes as a result of the SCID mutation. Consequently, human hepatocytes can be transplanted into these mice and establishment of these hepatocytes can compensate for damaged endogenous murine hepatocyte functions. Periodic intraperitoneal nafamostat mesilate injections are needed to maintain immunotolerance to the human hepatocytes.

To date, a few animal models containing human hepatocytes in the liver have been developed (Aurich et al., 2007; Dandri et al., 2001; Ho et al., 2005; Mercer et al., 2001; Meuleman et al.,

Address correspondence to: Yasushi Sato, Drug Safety and Pharmacokinetics Laboratories, Taisho Pharmaceutical Co., Ltd. 403, Yoshino-cho 1-chome, Kita-ku, Saitama City, Saitama, 331-9530, Japan; e-mail: yasushi.sato@po.rd.taisho.co.jp.

Abbreviations: uPA, urokinase-type plasminogen activator; SCID, severe combined immunodeficiency; APAP, acetaminophen; CK, cytokeratin; hAlb, human albumin; PCNA, proliferating cell nuclear antigen; TUNEL, TdT-dUTP nick end labeling; CYP, cytochrome P450; MRP, multidrug resistance protein; PGP, P-glycoprotein; PFA, paraformaldehyde; H&E, hematoxylin and eosin; IHC, immunohistochemistry; HRP, horseradish peroxidase; RI; replacement index; CAR, constitutive androstane receptor; NAPQI, N-acetyl-p-benzoquinone imine; HBV, hepatitis B virus; HCV, hepatitis C virus; KO, knockout; TG, transgenic.

TABLE 1.—Extent of human hepatocyte population in murine liver, by strain.

	uPA$^{+/+}$/SCID					
	RI < 30%	RI = 30–70%	RI > 70%	Total No.	uPA$^{WT/WT}$/SCID	uPA$^{+/-}$/SCID
Male (n)	7	3	3	13	2	2
RI-A	(0–25%)	(30–70%)	(>75%)		(0%)	(0%)
	(Avg 6.4%)	(Avg 50.0%)	(Avg 78.3%)			
RI-H	(0–28%)	(59–64%)	(72–85%)		(0%)	
	(Avg 3.7%)	(Avg 61.7%)	(Avg 80.0%)			(0%)
Female (n)	4	2	4	10	3	0
RI-A	(0–10%)	(50%)	(>80%)			
	(Avg 3.8%)	(Avg 50.0%)	(Avg 81.3%)		(0%)	(0%)
RI-H	(2–12%)	(46–48%)	(75–95%)			
	(Avg 7.3%)	(Avg 47.0%)	(Avg 84.5%)		(0%)	(0%)
Total (n)	11	5	7	23	5	2

Note: n: number of animals examined.

RI (replacement index): Percentage of human hepatocytes as estimated by blood hAlb level (RI-A) or positive immunohistochemical staining (CK8,18 or OCH1E5) human hepatocyte area, expressed as a percentage of the total liver section area (RI-H). Values in the parentheses represent the range of minimum and maximum RI as well as the average (Avg %).

2005; Ouyang et al., 2001). Most of these humanized liver models are not sufficiently populated with transplanted human hepatocytes and the normal hepatic architecture is not maintained or restored. In this study we characterized the morphologic and functional differentiation of transplanted human hepatocytes in the chimeric liver of uPA$^{+/+}$/SCID mice and evaluated their response to acetaminophen, a classical hepatotoxin.

MATERIALS AND METHODS

Chemical

Acetaminophen (APAP) was purchased from Sigma-Aldrich (St. Louis, MO, USA) and dissolved in 0.5% methylcellulose (Metolose SM-4000; Shin-Etsu Chemical, Tokyo, Japan) aqueous solution.

Treatment of Animals

To characterize the morphologic features of human hepatocytes in the chimeric mouse liver, 23 uPA$^{+/+}$/SCID mice with humanized livers (chimeric mice), 5 uPA$^{WT/WT}$/SCID mice, and 2 uPA$^{+/-}$/SCID mice were examined (Table 1). The toxicological responses to APAP were evaluated in 9 chimeric and 15 ICR (SLC Japan, Atsugi, Japan) mice. All experiments were conducted in accordance with the Hiroshima Prefectural Institute of Industrial Science and Technology Ethics Board, the Ethics Committees of Kanazawa University, and the Animal Ethics Committee of Pfizer Global Research and Development Nagoya Laboratories.

Chimeric mice with humanized livers were generated by the method described previously using uPA$^{+/+}$/SCID mice (Figure 1; Tateno et al., 2004). uPA$^{+/-}$ transgenic mice (B6SJL-TgN [Alb1Plau] 144Bri; The Jackson Laboratories, Bar Harbor, ME, USA) were crossed with SCID mice (Fox Chase SCID C.B-17/Icr-scid Jcl; Crea Japan, Tokyo, Japan) to generate uPA$^{+/+}$/SCID, uPA$^{+/-}$/SCID, and uPA$^{WT/WT}$/SCID mice. Human hepatocytes were purchased from In Vitro Technologies (Baltimore, MD, USA) or BD Gentest (Woburn, MA, USA). At 20–30 days of age, uPA$^{+/+}$/SCID mice were inoculated with human hepatocytes through a small left-flank incision into the inferior splenic pole. Following inoculation, human albumin (hAlb) was measured weekly in 2-μL tail vein blood samples using an enzyme-linked immunoassay kit (Bethyl Laboratories, Montgomery, TX, USA). To maintain immunotolerance to the transplanted

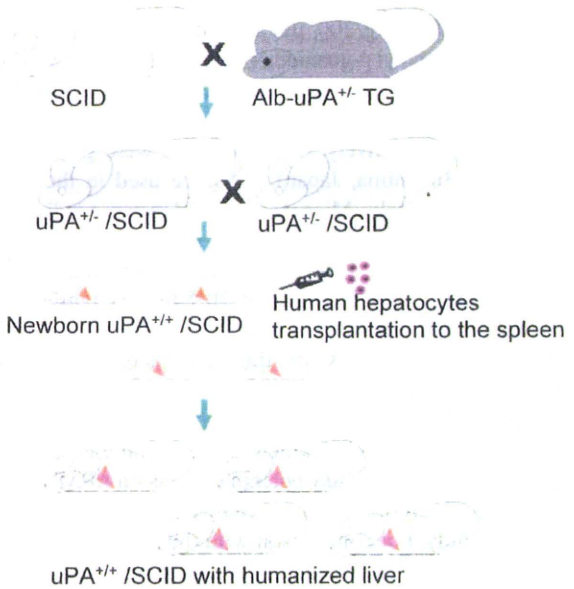

FIGURE 1.—Schematic showing the method by which urokinase-type plasminogen activator transgenic/severe combined immunodeficiency (uPA$^{+/+}$/SCID) mice with humanized livers were generated. A mouse heterozygous for the uPA transgene (albumin promoter; alb-uPA$^{+/-}$ TG) was crossed with a SCID mouse; uPA$^{+/-}$/SCID mice are then crossed. Newborn uPA$^{+/+}$/SCID mice receive an inoculation of human hepatocytes into the spleen. The mouse liver is then repopulated with transplanted human hepatocytes.

TABLE 2.—Summary of immunohistochemistry materials and methods.

Antigen	Source and type (clone or origin)	Tissue fixation and embedding	Dilution	Expected reactivity	Pretreatment
Human hepatocyte	Dako MoAb (OCH1E5)	Frozen (PFA or acetone)	1:100	Hepatocyte (H*)	None
CK8,18	Cappel MoAb (NCL503)	Frozen (acetone)	1:20	CK8,18 (H)	None
Human albumin	Bethyl PoAb (goat)	Frozen (PFA)	1:20	Albumin (H)	None
Laminin	Dako PoAb (rabbit)	Paraffin (PFA)	1:1	Laminin (H and M*)	Proteinase K
CD31	Dako MoAb (JC70A)	Paraffin (PFA)	1:50	CD31 (H and M)	Heat
PCNA	Dako MoAb (PC10)	Paraffin (PFA)	1:100	PCNA (H and M)	Heat
Human CYP3A4	Gentest PoAb (rabbit)	Frozen (acetone)	1:100	CYP3A4 (H)	None
Human CYP3A5	Gentest PoAb (rabbit)	Frozen (acetone)	1:50	CYP3A5 (H)	None
CYP2E1	CHEMICON PoAb (rabbit)	Paraffin (PFA)	1:50	CYP2E1 (H)	None
Human MRP2	MONOSAN MoAb (M2III-6)	Paraffin (PFA)	1:20	MRP2 (H)	Heat
Human MRP3	MONOSAN MoAb (M2III-6)	Paraffin (PFA)	1:20	MRP3 (H)	Heat
Human MRP6	MONOSAN MoAb (M2III-6)	Paraffin (PFA)	1:20	MRP6 (H)	Heat
PGP	Dako MoAb (C494)	Paraffin (PFA)	1:20	PGP (H and M)	Heat

Note: H*, human; M*, mouse; moAb, monoclonal antibody; poAb, polyclonal antibody.

human hepatocytes, uPA$^{+/+}$/SCID mice were injected intraperitoneally with 0.3 mg/200 μL/animal nafamostat mesilate (6-amidino-2-naphthyl p-guanidinobenzoate dimethanesulfonate; Torii Pharmaceutical, Tokyo, Japan) once every 2 days, once per day or twice per day for hAlb levels of up to 4 mg/mL, 6 mg/mL, or >6 mg/mL, respectively. Chimeric mice were generated by PhoenixBio (Hiroshima, Japan). All mice used in the studies were aged 11–14 weeks. Mice were housed in cages individually (175 × 245 × 125 mm) with free access to tap water and a pellet diet (CRF-1; CREA Japan, Tokyo, Japan). The animal room was maintained at 21–25°C with 40–70% relative humidity and a 12 h light-dark cycle.

For the APAP toxicity study, three groups of chimeric mice (12–14 weeks; n = 3/group, hAlb = 6.6–15.1 mg/mL) received a single dose of APAP by oral gavage (0 mg/kg, 1,400 mg/kg, and 1,400 mg/kg) and were killed at 24, 4, and 24 h postdose, respectively. To eliminate any potential effects on APAP toxicity, chimeric mice were not administered nafamostat in the 3 days prior to the study. For comparison with the chimeric mice, five groups of ICR mice (12 weeks; n = 3/group) were administered APAP by oral gavage (0 mg/kg, 400 mg/kg [two groups], and 1,400 mg/kg [two groups]) and killed at 4 or 24 h postdose. ICR mice were used in this experiment because sufficient uPA$^{WT/WT}$/SCID mice were not available from the bleeding scheme; in addition, the ICR strain is commonly used in toxicology study in Japan.

Necropsy and Tissue Preparations

Animals were killed by cutting the abdominal aorta after anesthesia with isoflurane (inhalation) or pentobarbital (70 mg/kg, intraperitoneal injection). Tissues were fixed in 4% paraformaldehyde (PFA) or snap-frozen in liquid nitrogen. PFA-fixed tissues were analyzed by light or electron microscopy, and frozen-tissue sections were used for specific immunohistochemical assays. For light microscopy, PFA-fixed samples were trimmed, embedded in paraffin, sectioned to a thickness of 4 μm, and stained with hematoxylin and eosin (H&E) or used in immunohistochemistry assays.

Immunohistochemistry

Immunohistochemistry (IHC) was used to demonstrate the expression of human proteins in transplanted hepatocytes, sinusoidal endothelial cells, and basement membranes. Markers of cell proliferation and apoptosis were also detected via IHC. Specific reagents and experimental conditions are summarized in Table 2. Frozen tissues were sectioned at 6 μm and mounted on glass slides, and postfixed in cold acetone or 4% PFA for 3 minutes and incubated with antibody. Additional PFA-fixed tissues were processed routinely, paraffin embedded, and sectioned at 6 μm. Pretreatment of paraffin tissue sections consisted of 0.01 M citric acid (pH 6.0) in distilled water at 100°C for 10 minutes (heat pretreatment, Table 2) or proteinase K (DakoCytomation, Tokyo, Japan) for 10 minutes. Murine monoclonal antibodies were detected with avidin-biotin (Vectastain Elite ABC; Vector Laboratories, Burlingame, CA, USA) while peroxidase-conjugated rabbit anti-goat immunoglobulin G (IgG; Chemicon, Temecula, CA, USA) or goat anti-rabbit IgG (Vectastain) for the rabbit polyclonal antibodies were used as the secondary antibodies. IHC stains were visualized with the chromogen 3,3′-diaminobenzidine tetrachloride (DakoCytomation) and counterstained with hematoxylin.

Detection of Apoptosis

The In Situ Apoptosis Detection Kit (TACS2 TdT-DAB; Trevigen, Gaithersburg, MD, USA) was used to label apoptotic cells in paraffin sections (TdT-dUTP nick end labeling or TUNEL). TUNEL labeling required pretreatment of the tissue sections with proteinase K, and Mn^{2+} was used as the cation in the labeling reaction mixture. Paraffin-embedded small intestine was used as the positive tissue control for the proliferating cell nuclear antigen (PCNA) and TUNEL staining.

Image Analyses

Quantitative image analysis was carried with the Image Processor for Analytical Pathology (IPAP-WIN; Sumika Technoservice, Osaka, Japan). The replacement index (RI), which is the extent of human hepatocyte population in the mouse liver, was expressed as the percentage of CK8,18- or OCH1E5-positive staining area in the total liver section. Immunolocalization of CYP expression (CYP% = percentage of CYP-positive area in the total liver section) and PCNA-labeling indices (PCNA-LI% = percentage of PCNA-positive cells in the liver section) were calculated. For each animal, four fields (4× objective for CK8,18 or OCH1E5, 10× for PCNA) were measured to calculate the average score for each IHC marker.

Electron Microscopic Examinations

For transmission electron microscopy, small pieces of PFA-fixed liver from three mice (one uPA$^{WT/WT}$/SCID and two chimeric mice with RI > 90%) were postfixed in 2.5% glutaraldehyde, contrasted with 1% osmium tetroxide, and embedded in epoxy resin. Sections were cut to a thickness of 1 µm, stained with toluidine blue, and examined microscopically. Appropriate areas were selected in the semithin sections, and ultrathin sections were made from the trimmed blocks. Ultrathin sections mounted on the grid mesh were stained with uranyl acetate and lead citrate, and observed with a Hitachi H-7600 electron microscope (Hitachi, Tokyo, Japan).

RESULTS

Histopathology of the Chimeric Mouse Livers

H&E and IHC analysis of the human hepatocyte markers demonstrated proliferation of human hepatocytes with varying degrees of replacement of mouse hepatocytes in the chimeric livers (Figure 2).

The livers from uPA$^{+/+}$/SCID chimeric mice exhibited multifocal clear eosinophilic areas interspersed with or surrounded by basophilic hepatocytes (Figure 2A, 2B, 2G, and 2H). In contrast, livers from uPA$^{WT/WT}$/SCID mice consisted of normal appearing hepatocytes (Figure 2C and 2I). The clear eosinophilic areas in the chimeric mice were positive for OCH1E5 (Figure 2F), CK8,18 (Figure 2D and 2E), and hAlb (Figure 2J and 2K) by IHC and were interpreted to represent viable, transplanted human hepatocytes. As shown in Table 1, chimeric mice had varying amounts of human hepatocytes in the liver (RI up to 95%), and the RI generally correlated with the hAlb levels in the blood (data not shown). In areas negative for hAlb, CK8,18, and OCH1E5 staining, basophilic small hepatocytes (replacing irregular areas of single-cell hepatocyte necrosis) and brown pigment-laden macrophages were observed. These histological features were distinct from those of uPA$^{WT/WT}$/SCID mice (Figure 2). In chimeric mice with lower RI, normal mouse hepatocytes were observed in the liver; furthermore, these normal murine hepatocytes were negative for human hepatocyte markers (Figure 2A). Thus, the chimeric mouse livers had three components: foci of repopulating human hepatocytes, degenerating donor mouse hepatocytes, and histologically normal mouse hepatocytes. Human hepatocytes in the chimeric livers were distinguished from murine hepatocytes by their clear cytoplasm and smaller nuclei on H&E staining (Figure 2). Furthermore, PCNA IHC demonstrated proliferation of human hepatocytes in the mouse liver. The human hepatocyte foci exhibited varying amounts of proliferation (PCNA labeling index [PCNA-LI], 22–68%) and apoptotic cells were observed in the murine hepatocyte areas (Figure 3). In well-differentiated foci of human hepatocytes (CK8,18 or OCH1E5 positive with low PCNA-LI), hepatic cords and sinusoid-like structures were observed (Figures 4E and 5A).

Laminin and CD31 IHC were used to evaluate the architecture of the human hepatocyte foci and the relationship with degenerating murine hepatocytes (Figure 4). In areas of degenerating mouse hepatocytes, the sinusoid structure was characterized by the presence of increased laminin positive filaments (Figure 4C). In the human hepatocyte areas, poorly vascularized hepatocyte aggregates (few CD31-positive sinusoid endothelial cells) were observed in the areas of proliferating (higher PCNA LI) human hepatocytes (Figure 4C and 4D). Developing hepatic cords were lined by a laminin–positive basement membrane and by CD31-positive sinusoid endothelial cells (Figure 4E and 4F).

Electron microscopy demonstrated developed bile canaliculi between human hepatocytes (Figure 5C and 5E). Furthermore, transplanted hepatocytes expressed CYP2E1 (predominantly diffuse, >70% hepatocytes, Figure 2M), CYP3A4 (faint and diffuse in >40% cells), and CYP3A5 (faint staining in <5% cells) proteins. In addition, IHC localized expression of the MRP2 transporter to the apical hepatocyte membrane (Figure 2N), with faint expression of MRP3 (Figure 2O), and MRP6 and P-glycoprotein (PGP; data not shown), in the basolateral membranes of the human hepatocytes.

Toxicological Responses to APAP

The toxicological response in the chimeric liver following APAP administration was compared with that of the ICR mouse liver (Figure 6), a standard toxicology strain in Japan. At 24 h postdose, all chimeric mice survived the oral administration of APAP at 1,400 mg/kg, while ICR mice were dead. In the livers of chimeric mice receiving 1,400 mg/kg APAP, mild vacuolation of hepatocytes (Figure 6E and 6F) and mild hepatocellular degeneration (Figure 6F) were observed in the human hepatocyte areas. A few TUNEL-positive cells were observed in the human hepatocyte area at 4 h after administration of 1,400 mg/kg APAP, but these were not apparent at the 24 h time point. CYP IHC revealed that APAP–related changes were limited to a 63% decrease (relative to vehicle control) in CYP2E1 expression at 24 h (Figure 6J–L). APAP hepatotoxicity was mild in the chimeric mouse livers, in contrast to the severe centrilobular hepatocellular necrosis observed in the ICR mouse livers (Figure 6N and 6O). These results suggest that the chimeric mice are less susceptible to APAP toxicity than ICR mice. This may be due to differences between human and mouse hepatocytes, genetic differences between the uPA$^{+/+}$/SCID and ICR mice strains, or some combination of these two factors.

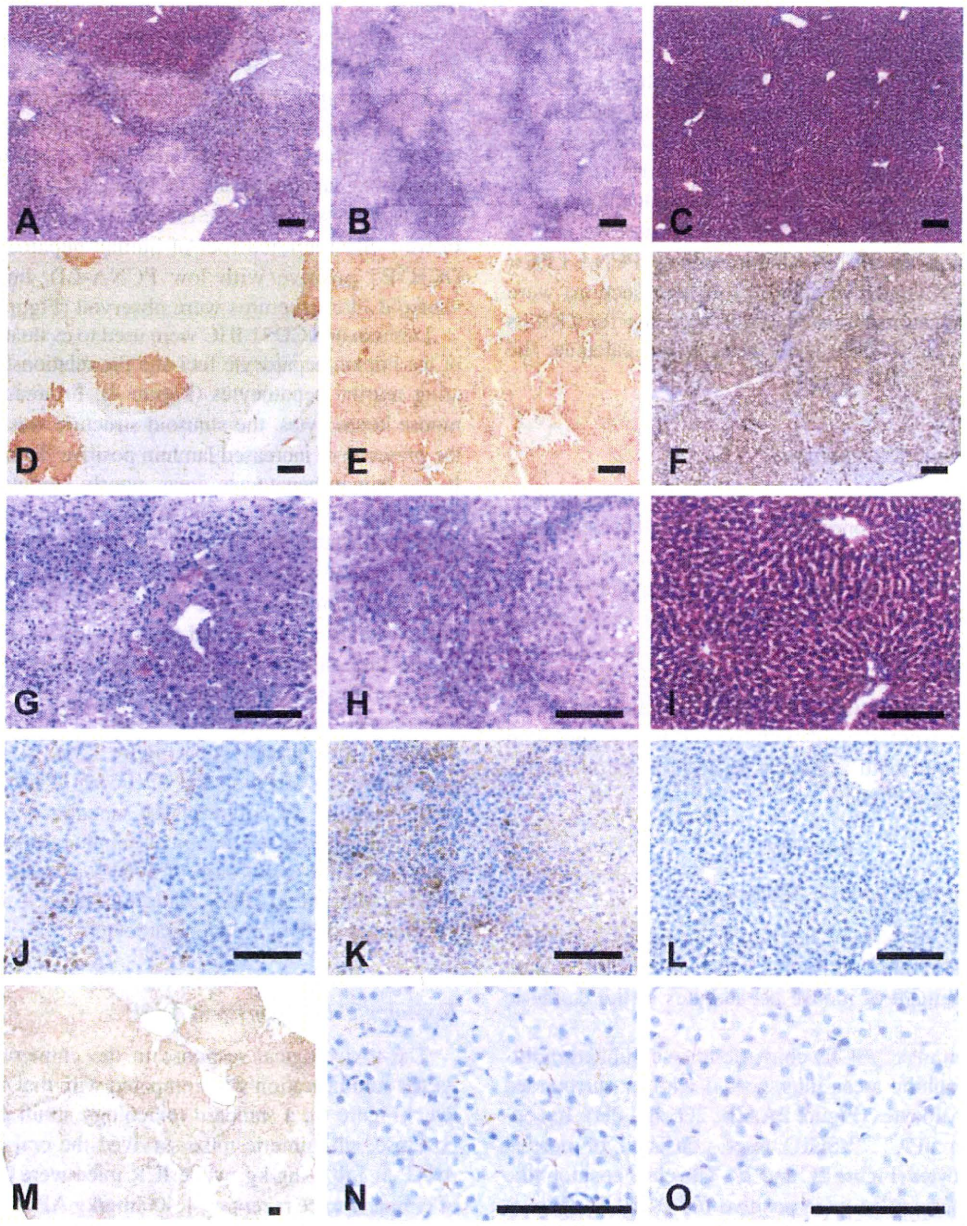

FIGURE 2.—Histopathological characterization of the livers of urokinase-type plasminogen activator transgenic/severe combined immunodeficiency (uPA$^{+/+}$/SCID) chimeric mice and uPA$^{WT/WT}$/SCID mice. Eosinophilic clear foci were observed in the uPA$^{+/+}$/SCID chimeric mouse livers with lower RI (A and G: RI = 56%, hAlb = 2.1 mg/mL) and higher RI (B and H: RI = 87%, hAlb = 10.8 mg/mL), whereas livers of the uPA$^{WT/WT}$/SCID mice appeared normal (C and I) with hematoxylin and eosin staining. Areas of normal hepatocytes were observed in the lower RI chimeric mouse (A, upper left). Clear foci were positive for immunohistochemical markers for human hepatocytes: CK8,18 (D and E, corresponding to A and B, respectively), OCH1E5 (F, corresponding to B/E), and hAlb (J and K, corresponding to G and H, respectively). The uPA$^{WT/WT}$/SCID mouse liver was negative for hAlb immunostaining (L, corresponding to I). Results of immunohistochemical analyses of human CYP2E1 (predominantly diffuse pattern; M), MRP2 (apical hepatocyte membrane; N), and MRP3 (faint basolateral membrane; O) in chimeric liver are also shown. WT, wild type; RI, replacement index; hAlb, human albumin. Bar = 100 μm.

DISCUSSION

In the present study, mouse-human chimeric livers contained variable numbers of human hepatocytes as demonstrated by IHC with human-specific hepatocellular markers and circulating hAlb. Human hepatocytes proliferated extensively (PCNA-LI, 22–68%) in the mouse liver, replacing damaged and degenerating murine hepatocytes and restoring some of the architectural

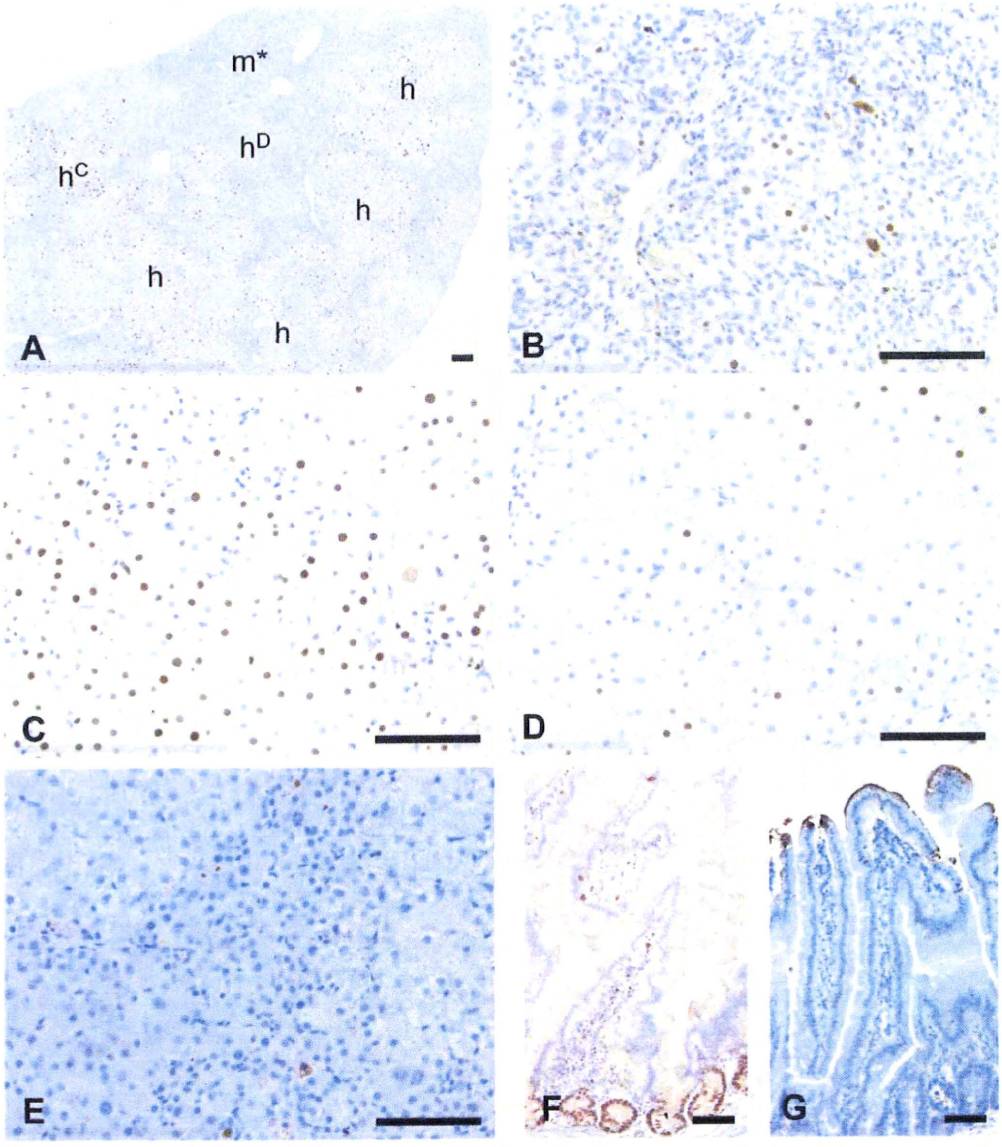

FIGURE 3.—Cell proliferation and apoptosis in the liver of an urokinase-type plasminogen activator transgenic/severe combined immunodeficiency (uPA$^{+/+}$/SCID) chimeric mouse with a replacement index (RI) of 85%. Proliferating cell nuclear antigen (PCNA) immunohistochemistry revealed proliferating human (h) hepatocyte foci in the mouse (m) liver (A). PCNA labeling index (LI) of the mouse area was 25% (B, corresponding to m* in Figure 2A). Human hepatocyte foci indicate proliferating areas (C: PCNA-LI = 64%, corresponding to h^C in Figure 2A) and differentiating areas (D: PCNA-LI = 22%, corresponding to h^D in Figure 2A). TUNEL-positive apoptotic cells were observed in the mouse area (E). Positive controls of small intestine samples for PCNA (F) and TUNEL (G) are also shown. TUNEL, TdT-dUTP nick end labeling. Bar = 100 μm.

features (bile caniliculi, sinusoidal endothelial cells, basal lamina). The chimeric mouse with the highest hAlb levels appeared healthy, except for small body size, as previously described (Tateno et al., 2004). In addition, the livers did not exhibit any inflammatory reactions associated with the presence of the human hepatocytes (Tateno et al., 2004).

The results described here suggest that the transplanted human hepatocytes can function effectively in terms of nutrition, bile acid secretion, and synthesis of hAlb or other proteins without adversely affecting the donor mouse. Furthermore, in the murine environment, these human hepatocytes retained expression of human CYPs and transporter proteins (Katoh and Yokoi, 2007; Nishimura et al., 2005; Tateno et al., 2004; Tsuge et al., 2005) and can be expected to retain human liver function. Although the light and electron microscopic features of the humanized hepatocyte areas showed incompletely developed architecture, sinusoid-like CD31-positive vascular channels, hepatic cord-like structures, and bile canaliculi were observed in the well-differentiated human hepatocyte areas.

Mouse hepatocytes undergoing replacement by transplanted human hepatocytes appeared shrunken and degenerate, similar to those reported in Alb-uPA$^{+/+}$ transgenic mice (Sandgren et al.,